

# Changes in spectral properties and composition of lipofuscin fluorophores from human-retinal-pigment epithelium with age and pathology

Tatiana B. Feldman · Marina A. Yakovleva · Patimat M. Arbukhanova ·  
Sergey A. Borzenok · Alexey S. Kononikhin · Igor A. Popov · Evgeny N. Nikolaev ·  
Mikhail A. Ostrovsky

Received: 22 September 2014 / Revised: 16 November 2014 / Accepted: 17 November 2014 / Published online: 4 December 2014  
© Springer-Verlag Berlin Heidelberg 2014

**Abstract** Fundus autofluorescence mostly originates from bisretinoid fluorophores in lipofuscin granules, which accumulate in retinal-pigment-epithelium cells with age. The dynamics of accumulation, photo-oxidation, and photodegradation of bisretinoids during aging or in the presence of pathology have been insufficiently investigated. Changes in spectral properties and composition of human lipofuscin-granule fluorophores with age and pathology have now been investigated by a high-performance liquid chromatography method using spectrophotometric and fluorescent detectors connected in series. It was found that: (i) *N*-retinylidene-*N*-retinylethanolamine (A2E) fluorescence

intensity is not predominant in the chloroform extract of human-cadaver-eye retinal pigment epithelium studied; bisretinoid photo-oxidation and photodegradation products have much higher fluorescent properties; (ii) the relative emission maximum in the fluorescence spectrum of suspended retinal-pigment-epithelium cells obtained from an individual human-cadaver eye without pathology is irrespective of donor age and falls within the range  $575 \pm 15$  nm; in two cadaver eyes with signs of age-related macular degeneration, emission maxima were shifted by 23–36 nm towards the shortwave region; and (iii) the ratio of bisretinoid photo-oxidation and photodegradation products to unoxidized bisretinoids in the chloroform extract of cadaver-eye retinal pigment epithelium increases with donor age, from  $0.69 \pm 0.03$  to  $1.32 \pm 0.04$ . The differences in fluorescence properties between chloroform extracts obtained from cadaver eyes with and without signs of age-related macular degeneration could be used to increase the potential of fundus autofluorescence imaging as a noninvasive diagnostic method.

T. B. Feldman (✉) · M. A. Ostrovsky  
Department of Molecular Physiology, Biological Faculty,  
Lomonosov Moscow State University, Leninskie Gory1,  
Moscow 119991, Russia  
e-mail: feldmantb@mail.ru

T. B. Feldman · M. A. Yakovleva · I. A. Popov · E. N. Nikolaev ·  
M. A. Ostrovsky  
Emanuel Institute of Biochemical Physics, Russian Academy of  
Sciences, Kosygin st.4, Moscow 119334, Russia

P. M. Arbukhanova · S. A. Borzenok  
Sv. Fyodorov Eye Microsurgery Complex, Beskudnikovsky bld.  
59a, Moscow 127486, Russia

A. S. Kononikhin · E. N. Nikolaev  
Institute for Energy Problems of Chemical Physics, Russian  
Academy of Sciences, Leninsky pr. 38 bld. 2, Moscow 119 334,  
Russia

A. S. Kononikhin · I. A. Popov · E. N. Nikolaev  
Moscow Institute of Physics and Technology, Institutsky per. 9,  
Dolgoprudnyi, Moscow Region 141700, Russia

E. N. Nikolaev  
Orekhovich Institute of Biomedical Chemistry, Russian Academy of  
Medical Sciences, Pogodinskaya st. 10, Moscow 119121, Russia

**Keywords** Retinal pigment epithelium · Lipofuscin granule ·  
Bisretinoid fluorophores · Fundus autofluorescence ·  
High-performance liquid chromatography

## Introduction

Noninvasive fundus autofluorescence (AF) imaging is based on AF of lipofuscin granules (LGs) in retinal-pigment-epithelium (RPE) cells [1]. LGs are formed as a result of incomplete lysosomal degradation of outer-segment photoreceptor-cell debris [2]. They accumulate in RPE with age, accumulating particularly intensively in patients with hereditary diseases including recessive Stargardt disease [3], Best vitelliform macular dystrophy [4], and progressive age-related

macular degeneration (AMD) [5, 6]. LGs contain bisretinoids, which are byproducts of the photolysis of the visual pigment rhodopsin. All-*trans*-retinal derivatives are the main source of LG fluorescence and determine LG phototoxic properties [7, 8].

Investigation of the composition, spectral characteristics, and contribution to fundus AF of LG fluorophores is one way of increasing the information value of the fundus-AF imaging method [9]. The composition of fluorophores in LGs may change with age or in the presence of pathology which, in turn, may lead to a change of fundus-AF spectral characteristics [10]. Determination of the correlation between fluorophore composition in LG and AF spectral properties might become an additional indicator of pathology development.

Fluorescent LG properties are determined by the presence of 21 fluorophores [11, 12]. *N*-retinylidene-*N*-retinylethanolamine (A2E) has been studied in some depth [13, 14]. A2E is formed from its precursor, *N*-retinylidene-*N*-retinyl-phosphatidylethanolamine (A2PE), in RPE lysosomes via enzymatic cleavage of the phosphoether bond [15]. A2PE is the product of the attachment of two all-*trans*-retinal moieties to the amino group of one of the photoreceptor membrane lipids, phosphatidylethanolamine [16, 17]. As well as A2E, a series of all-*trans*-retinal conjugates in LGs have been characterized [18–21]. Photo-oxidation and photodegradation products of bisretinoids (A2E<sub>ox,deg</sub>), which are highly reactive aldehydes and ketones, have been investigated [22–24]. These products are rather toxic. The composition of LG fluorophores, especially their photooxidation products and contribution to total fluorescence intensity in the presence or absence of pathology, has not been determined.

Compositional analyses of LG fluorophores identify A2E as a major component in RPE [25, 26]. However, the contribution of different LG fluorophores to fundus AF is not known. Investigations give grounds to assume that the main LG fluorophore A2E is not predominant in total LG fluorescence, and therefore does not make the greatest contribution to the total intensity of fundus AF. For instance, it has been concluded that oxidized forms of A2E have stronger fluorescence than A2E itself [20, 27, 28].

This paper reports the application of HPLC to a thorough fluorescent analysis of all detectable fluorophores in RPE chloroform extract from human-cadaver eyes. It is revealed that the fluorescence intensity of A2E and iso-A2E, recorded in the extract studied at different excitation and emission wavelengths, is much lower than that of other fluorophores. An age-related change in the ratio of detectable fluorophores in RPE chloroform extracts obtained from cadaver eyes without signs of pathology is revealed. Comparative analysis of the relative content of fluorophores in RPE chloroform extract from cadaver eyes with and without signs of AMD reveals differences between them.

## Materials and methods

### Ethical statement

Experiments on tissue isolated from human-cadaver eyes were performed in compliance with officially accepted procedures, in particular Russian Federation law N 4180-I dated 22.12.1992, “On human organs or tissue transplantation” (with modifications and additions dated 20.06.2000, 16.10.2006, 09.02.2007, and 29.11.2007); section II “Removal of organs or tissue from dead bodies”; clause 8 “Presumption of consent for removal of organs or tissue”; clause 10 “Permission to remove organs or tissue from dead bodies”. According to section II (clause 8) of this law, consent from the donor or the next of kin to use organs or tissue is not required [29].

On the basis of the Russian Federal Service on Surveillance in Healthcare (Roszdravnadzor) licenses No. 99-01-005317 dated 30.04.2008 and No. FS-99-01-008251 dated 18.02.2013, the Eye Tissue Bank located in the Sv. Fyodorov Eye Microsurgery Complex (Beskudnikovskiy bld. 59a, Moscow, Russia, 127486, [http://www.mntk.ru/mntk-moscow/Scientific-units/biology/glaznoy\\_bank/](http://www.mntk.ru/mntk-moscow/Scientific-units/biology/glaznoy_bank/)) obtains human-cadaver eyes from the mortuary departments of the Moscow Forensic Medical Examination Bureau. These licenses permit the use of tissue isolated from human-cadaver eyes for transplantation and scientific research.

Permission was obtained from the chief medical officer of the Sv. Fyodorov Eye Microsurgery Complex, under a scientific collaboration agreement between the Complex and the Emanuel Institute of Biochemical Physics dated 11.01.2011, to perform scientific research in the Laboratory of Physical and Chemical Bases of Vision at the Institute with RPE from cadaver eyes.

Cadaver eyes, after removal of corneas for transplantation, were delivered by the Eye Tissue Bank to the Laboratory by road in a box for human organs. Cadaver eyes after isolation of RPE were returned to the Eye Tissue Bank for use, in compliance with officially accepted procedures.

### Chemicals

Chemicals used in the experiments were of recognized analytical grade and commercially available. All solvents used were HPLC grade and were purchased from Sigma and Fluka. Reagents were purchased from Sigma, Sigma–Aldrich, Fluka, and Merck.

### Tissues

Human-cadaver eyes were obtained from the Eye Tissue Bank within 10 h of donor death. Every cadaver eye was subject to post-mortem inspection by an ophthalmologist. For every

sample, an inspection procedure required indication of the age and sex of the donor, and a detailed description of the fundus before and after removal of the retina. Moreover, after retina removal, photos of the fundus were taken (see “Results” section).

All stages of sample preparation were performed under subdued lighting.

#### Preparation of suspended RPE cells from cadaver eyes

An incision into the sclera of the cadaver eyes was made with scissors, and the iris, lens, vitreous body, and retina were removed. The eyecup with the naked RPE layer was added to 1 mL 0.1 mol L<sup>-1</sup> phosphate buffer (pH 7.2–7.4). A microsurgical spatula was then used to cause desquamation of the RPE surface from the macula zone. The cell suspension was aspirated into a disposable pipette and transferred to a cooled flask.

#### Preparation of chloroform extracts from cadaver-eye RPE

The soluble fraction was extracted from the samples with an organic solvent by the Folch method [30]. A twofold excess of chloroform–methanol (2:1) mixture by volume was added to the RPE suspension described in the previous section, and the mixture was agitated with an electrical stirrer for 2 min and then incubated for 10 min at 4 °C. The mixture was then centrifuged (680g, 10 min, 4 °C). The bottom chloroform phase was aspirated into a syringe and transferred to a flask. The chloroform extract obtained was evaporated using a vacuum pump (Vacuubrand MZ 2CNT+AK+M+D, Germany). For further chromatographic analysis, each dried sample was resuspended in 200 µL methanol.

#### HPLC

The compound was passed through a Knauer chromatography system (Germany) equipped with a Kromasil-100-5-C18 (4 × 250 mm, sorbent size 5 µm) column. HPLC analysis was performed using a reverse-phase gradient from 80 % acetonitrile–20 % water (+0.05 % TFA) by volume to 100 % acetonitrile for 20 min at a flow of 1.0 mL min<sup>-1</sup>.

Absorbance (K-2501 detector, Knauer) and fluorescence (RF-10A-xl fluorescence detector, Shimadzu) were detected at specific wavelengths. The fluorescence detector was connected in series with the spectrophotometric detector of the chromatography system. Absorbance and fluorescence efficiency were estimated as peak areas (mV s) using the EuroChrom 5.05 chromatographic program. Precision for each sample was determined from three separately measured chromatograms for each individual sample. The surface area of each component in the mixture was calculated as a percentage of total surface area of all peaks, i.e., the relative content of

each component. Most detectable products are unknown, and hence their fluorescent properties and relative contents were estimated regardless of extinction factors. The linear distribution was obtained by data processing, and thus the Student’s *t*-test was chosen for further calculations of reliability.

#### LG-chloroform-extract samples for HPLC absorption and fluorescence component analysis

Three chloroform extracts of suspended RPE cells from cadaver eyes with no signs of pathology were obtained:

- Sample 1, from eight cadaver eyes from donors aged 34 years (*n*=2) and 35 years (*n*=6);
- Sample 2, from seven cadaver eyes from donors aged 23 years (*n*=2), 25 years (*n*=2), 30 years (*n*=1), and 31 years (*n*=2); and
- Sample 3, from five cadaver eyes from donors aged 38 years (*n*=2), 40 years (*n*=2), and 41 years (*n*=1).

Tables 2 and 3 show a statistical analysis of results obtained for the three samples.

Samples for relative content of fluorophores in chloroform extract from cadaver eyes without signs of pathology, obtained from donors of different ages

Chloroform extracts from 42 cadaver eyes of donors aged 17 to 78 years, with no signs of pathological change in their RPE, were obtained and then analyzed by HPLC (reversed-phase, C<sub>18</sub> column). For each sample, the relative content of each detectable product was calculated from the chromatograms obtained. For statistical analysis, data on relative content of the individual products in the RPE extract analyzed were divided into groups by age:

- Group 1: 17 years (*n*=4), 20 years (*n*=2), 22 years (*n*=3), 24 years (*n*=2), and 27 years (*n*=1);
- Group 2: 30 years (*n*=1), 34 years (*n*=1), 35 years (*n*=2), 37 years (*n*=2), 38 years (*n*=1), and 39 years (*n*=1);
- Group 3: 40 years (*n*=2), 45 years (*n*=2), and 48 years (*n*=2);
- Group 4: 51 years (*n*=3), 54 years (*n*=1), 57 years (*n*=1), and 59 years (*n*=1);
- Group 6: 60 years (*n*=1), 61 years (*n*=1), 65 years (*n*=1), and 67 years (*n*=2);
- Group 8: 70 years (*n*=2), and 78 years (*n*=3).

Each group number corresponds to the column number in Fig. 4 and in Table 4.

Samples for relative content of fluorophores in RPE chloroform extract from cadaver eyes with signs of AMD

Inspection by an ophthalmologist detected two cadaver eyes with signs of AMD in the RPE, from donors aged 58 and 70 years.

Two individual samples of chloroform extract from suspended cadaver-eye RPE cells were obtained. These extracts were analyzed by HPLC (reversed-phase,  $C_{18}$  column), and the relative content of detectable products for each sample was calculated from the chromatograms obtained (Fig. 4 and Table 4, data in columns 5 and 7).

#### A2E synthesis and A2E photo-oxidation

A2E was prepared from all-*trans*-retinal and ethanolamine in acetic acid and ethanol, as described by Parish et al. [16]. The purity of A2E and iso-A2E was monitored by HPLC.

A2E (in acetonitrile) was irradiated for 2 h under constant stirring using a 150 W incandescent lamp (KGM 24-150, 400–700 nm) with a heat filter. The luminous flux density irradiating the sample was  $280 \text{ W m}^{-2}$  for visible light (400–700 nm), determined by photometer (Spectra-Physics 407A, USA).

A2E and products of its photo-oxidation were identified using a 7 T LTQ FT mass spectrometer (Thermo Electron Corp., Germany) equipped with an electrospray ion source, as described in [31]. The mass spectra were processed and analyzed using Qual Browser 1.4 software.

#### Spectroscopy

Absorption spectra were recorded on a Shimadzu UV-1700 spectrophotometer (Japan). Fluorescence-data acquisition was performed by means of an RF-5301 PC fluorimeter (Shimadzu, Kyoto, Japan) equipped with an R955-photomultiplier-tube detector (Hamamatsu, Shizuoka, Japan). RFPC software version 2.0 (Shimadzu) was used to compile the data. Emission spectra were recorded at 430 nm excitation with a sampling interval of 1 nm. The fluorescence spectra were corrected for the excitation intensity by the spectral response (quantum efficiency) of the R955-photomultiplier-tube detector. All fluorescence spectra were normalized to the maximum fluorescence intensity. The analysis was based on assessment of changes in locations of emission maxima.

## Results and discussion

#### HPLC analysis of synthetic A2E and A2E irradiation products

Synthetic A2E in acetonitrile was irradiated to obtain  $A2E_{ox,deg}$  products, to compare them with the products

contained in chloroform extracts from cadaver-eye RPE. Irradiation of A2E with visible light for 2 h causes its photo-oxidation and generation of new products (Fig. 1). The A2E absorption spectrum before irradiation (Fig. 1a, curve 1) has two characteristic maxima at 330 and 435 nm. A2E irradiation was accompanied by a substantial decrease in both of these maxima and the occurrence of a shorter-wavelength maximum at 280 nm (Fig. 1a, curve 2).

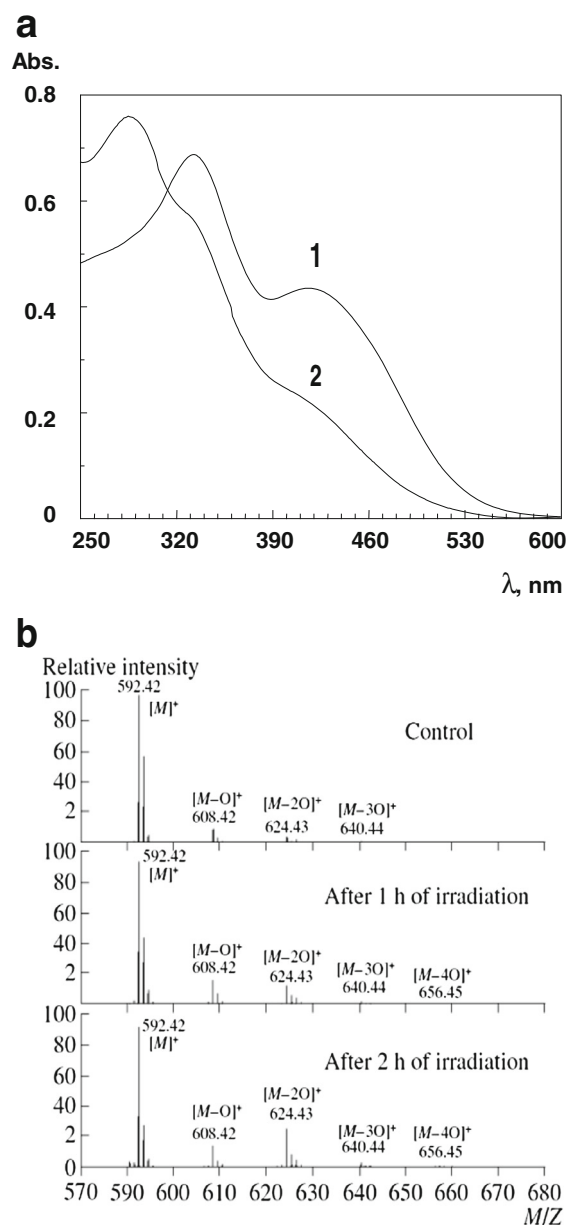


**Fig. 1** Synthetic A2E and products of its irradiation. Absorption spectra of A2E (a) in acetonitrile (1) and products of A2E after irradiation for 2 h with visible light (2). Mass spectra of compound A2E before and after irradiation with visible light (b). Designations:  $[M]^+$ , the major peak with  $m/z = 592$  corresponding to the unoxidized form of the molecular ion of A2E;  $[M-O]^+$ , the major peak plus oxygen: singly oxidized A2E ( $m/z = 608$ ), doubly oxidized A2E ( $m/z = 624$ ), triply oxidized A2E ( $m/z = 640$ ), and quadruply oxidized A2E ( $m/z = 656$ )

After sample irradiation, oxidized forms of A2E (oxy-A2E) were identified by mass spectrometry (Fig. 1b). In addition to the major peak with  $m/z = 592$  ( $M^+$ ), which corresponds to the unoxidized form of the A2E molecular ion, new peaks occurred. According to [8, 31, 32], these peaks correspond to singly oxidized A2E ( $m/z = 608$ ), doubly oxidized A2E ( $m/z = 624$ ), triply oxidized A2E ( $m/z = 640$ ), and quadruply oxidized A2E ( $m/z = 656$ ). As irradiation duration increases, the number of oxidized-A2E forms increases with respect to the unoxidized form, as indicated by the relative increase in intensity of peaks with  $m/z$  ratios of 608, 624, 640, and 656 compared with the peak with  $m/z = 592$ .

A comparative HPLC analysis of synthetic A2E and products formed during its irradiation was performed with absorption detection at a wavelength of 430 nm (Fig. 2). Photo-oxidation of A2E is accompanied by formation of several new products with shorter retention times. Figure 2a (chromatogram 1) shows HPLC data for synthetic A2E. The relative content of A2E and iso-A2E in the sample studied is ~87 % (Table 1). A2E<sub>ox,deg</sub> products detected at shorter retention times are present (Fig. 2b, chromatogram 1). Table 1 shows that after irradiation, the relative content of A2E and iso-A2E decreases to 10 %. It cannot be ruled out that each new product is a mixture of isomers or compounds with very

**Table 1** Relative content of synthetic A2E, iso-A2E, and products of A2E photo-oxidation and photodegradation before and after irradiation with visible light for 2 h<sup>a</sup>

Synthetic A2E	A2E <sub>ox,deg</sub> (%)	A2E and iso-A2E (%)	A2E <sub>mod</sub> (%)
Dark A2E	6.72±0.12	86.80±5.21	6.48±0.23
Irradiated A2E, 2 h	65.61±4.32	10.11±0.71	24.33±1.05

<sup>a</sup> Data were calculated from chromatograms in Fig. 2 (a and b, chromatograms 1)

similar properties. As well as the formation of these new products, a decrease in the amount of A2E is observed. This is another proof that the formation of these new products is a result of A2E chemical reactions.

Three groups of detectable substances can be identified on the chromatograms (Fig. 2b, chromatogram 1). The first group (A2E<sub>ox,deg</sub>) includes substances detected at the earliest times of product detection, including oxidized A2E products (oxy-A2E). The second group contains A2E and iso-A2E [16, 31]. The third group (A2E<sub>mod</sub>) may include products of A2E modification that are bisretinoids [18–20].

Figures 2a,b (chromatograms 2 and 3) show HPLC results of fluorescence-excitation analysis at a wavelength of 430 nm

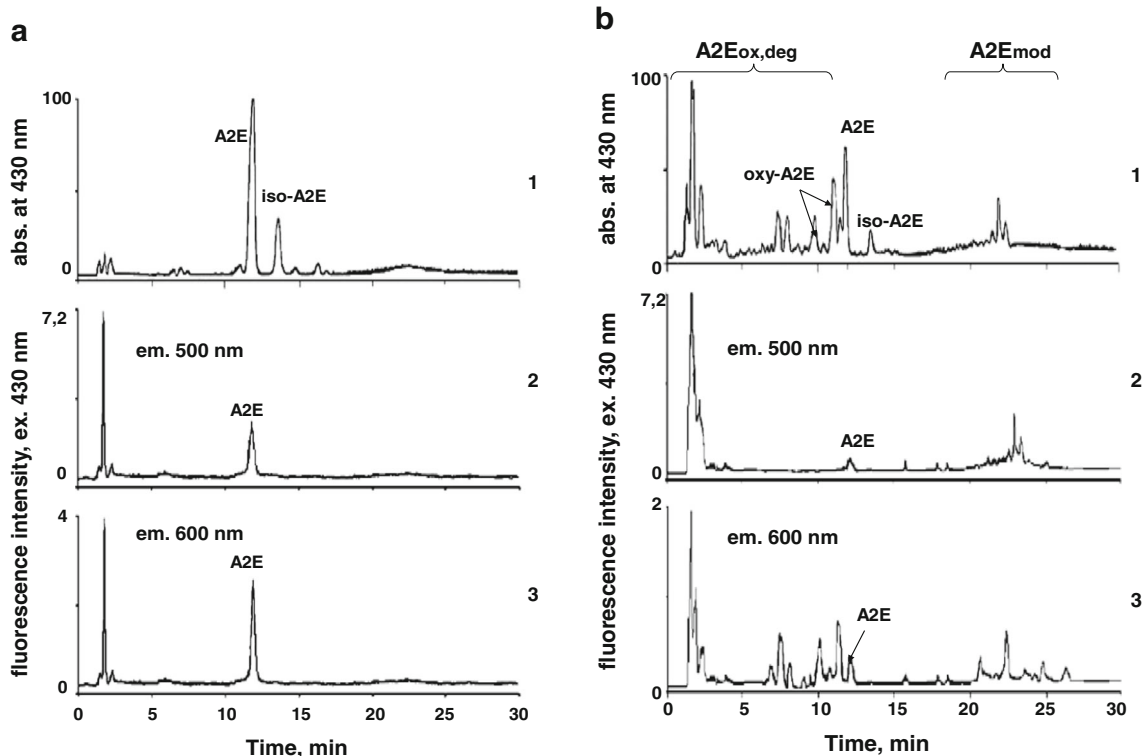


**Fig. 2** HPLC analysis of synthetic A2E and products of its irradiation. HPLC analysis of synthetic A2E (a). HPLC analysis of A2E products after irradiation with visible light for 2 h (b). Comparative HPLC analysis (C<sub>18</sub> column, reversed-phase gradient from 80 % acetonitrile–20 % water (+0.05 % TFA) by volume to 100 % acetonitrile for 20 min at a flow of

1.0 mL min<sup>-1</sup>) was performed using spectrophotometric and fluorescent detectors connected in series. 1, chromatograms with absorption detection at 430 nm; 2 and 3, chromatograms with fluorescence detection. Emission excitation was performed at 430 nm. Emission detection was monitored at 500 and 600 nm

and emission detection at 500 and 600 nm. The fluorescence intensity of non-irradiated A2E is significantly lower compared with its absorption. It is notable that iso-A2E has virtually no fluorescent properties. Also, the fluorescence intensity of all A2E products occurring after visible-light irradiation is higher than the fluorescence intensity of A2E itself.

#### HPLC absorption and fluorescence-component analysis of RPE chloroform extract

For comparative analysis of the fluorescence properties of individual fluorophores, total RPE chloroform extract was prepared from five to eight cadaver eyes from similarly aged donors without obvious signs of pathology in the RPE. HPLC analysis was performed using spectrophotometric and fluorescent detectors in series. The volume of a single sample was sufficient to record the absorption of individual components in the product mixture at different wavelengths and for fluorescence analysis at different fluorescence and emission excitation wavelengths. Therefore, all chromatograms obtained during component detection contain data on their composition and their individual contribution to fluorescence.

Figures 3a,b,c show chromatograms obtained by absorption detection (chromatogram 1) and fluorescence (chromatograms 2 and 3). Absorption was monitored at wavelengths of 340, 430, and 510 nm (a, b, and c, respectively), where most bisretinoids absorb [14, 18–21]. Fluorescence was excited by radiation at wavelengths of 340, 430, and 510 nm. Emission was detected at 500 and 600 nm for 340 and 430 nm excitation (a and b) and at 600 and 650 nm for 510 nm excitation (c). Figure 3 reveals that the highest absorption intensity of all detectable components of the chloroform extract is observed at 340 nm (a, chromatogram 1). On average, it decreases twofold at 430 nm (b, chromatogram 1) and nearly fourfold at 510 nm (c, chromatogram 1), as compared with the first chromatogram. Note also that the number of detectable products in each group decreases with increased detection wavelength.

Three groups of detectable substances can be distinguished on these absorption-detection chromatograms. The first group ( $A2E_{ox,deg}$ ) comprises substances detected at the earliest times, including oxidized-A2E products. There is a good correlation with  $A2E_{ox,deg}$ , shown on the chromatogram of A2E irradiation products (Fig. 2b, chromatogram 1), especially for products with retention times shorter than 5 min. The absorption spectra of  $A2E_{ox,deg}$  (Fig. 3d) also correlate with the absorption spectrum of A2E irradiation products (Fig. 1a, spectrum 2). The second group contains A2E and iso-A2E [16, 31]. The third group ( $A2E_{mod}$ ) includes products of A2E modification that could be bisretinoids [18–20]. This last group correlates with the third group on the A2E-irradiation-product chromatogram (Fig. 2b, chromatogram 1).

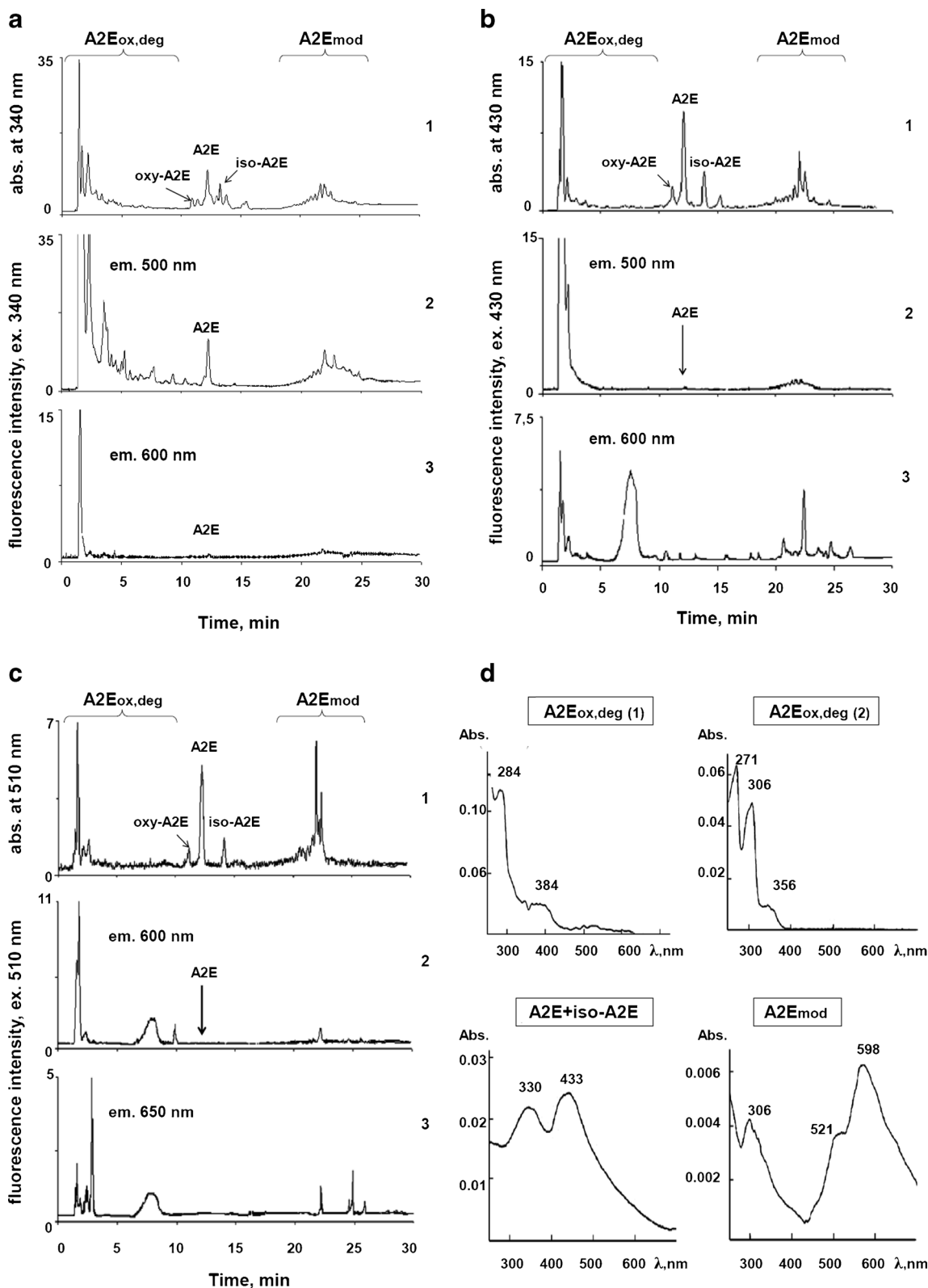
**Fig. 3** HPLC analysis of chloroform extracts from human RPE, obtained from eight cadaver eyes with no signs of pathology in the fundus, from subjects aged 34 years ( $n=2$ ) and 35 years ( $n=6$ ). Comparative HPLC analysis ( $C_{18}$  column, reversed-phase gradient from 80 % acetonitrile–20 % water (+0.05 % TFA) by volume to 100 % acetonitrile for 20 min at a flow of  $1.0 \text{ mL min}^{-1}$ ) was performed using spectrophotometric and fluorescent detectors connected in series. Chromatograms with absorption detection at 340 (a, 1), 430 (b, 1), and 510 (c, 1) nm. Chromatograms with fluorescence detection (a, b, and c (2 and 3)). Emission excitation was performed at 340 (a, 2, and 3), 430 (b, 2, and 3), and 510 (c, 2, and 3) nm. Emission detection was monitored at 500, 600, and 650 nm. Absorption spectra of fractions obtained during HPLC analysis (d).  $A2E_{ox,deg}$  (1) corresponds to the group of peaks 1 in Fig. 4a;  $A2E_{ox,deg}$  (2) corresponds to the group of peaks 2 in Fig. 4a; ( $A2E$ +iso-A2E) corresponds to the group of peaks 6–8 in Fig. 4a;  $A2E_{mod}$  corresponds to the group of peaks 11 in Fig. 4a

To measure absorption spectra, fractions from all three groups were isolated (Fig. 3d). The fractions of the  $A2E_{ox,deg}$  group (Figs. 3d, 1 and 2) absorb in the UV region and correlate with the A2E-irradiation-product absorption spectrum (Fig. 1a, spectrum 2). Absorption-spectrum maxima of the second fraction (Fig. 3d,  $A2E$  + iso-A2E) are the same as for synthetic A2E (Fig. 1a, spectrum 1). The fraction from the third group ( $A2E_{mod}$ ) comprises substances absorbing both in the short wavelength (close to 300 nm) and long wavelength (500–600 nm) regions (Fig. 3d,  $A2E_{mod}$ ).

Table 2 lists data on the relative content of mixture components in each group at different absorption wavelengths. Table 2 also indicates that the relative contribution of A2E and iso-A2E to total absorption of all detectable products in the RPE chloroform extract at different detection wavelengths is less than that of other groups.

Consider the chromatograms obtained by fluorescence detection (Figs. 3a,b,c, chromatograms 2 and 3). It is evident that the fluorescence intensity for the first group of peaks ( $A2E_{ox,deg}$ ) is much higher than that of all other components of the RPE chloroform extract, irrespective of the fluorescence excitation wavelength and the emission detection wavelength. The relative contribution of the  $A2E_{ox,deg}$  group to the total fluorescence of all detectable products has an average of 81–96 % (Table 3). The highest emission intensity on the chromatogram is observed for fluorescence excited by radiation of wavelength 340 nm (Fig. 3a, chromatogram 2). The fluorescence intensity for the  $A2E_{ox,deg}$  group at 500 nm gives ~96 % of the total contribution of the components (Table 3), whereas A2E gives only ~1 %. This correlates well with results from our earlier work [28].

When fluorescence is excited by radiation of wavelengths 430 and 510 nm and emission is detected at 500, 600, and 650 nm, the fluorescence intensity of all detectable products, and of their absorption, decreases rather abruptly. Moreover, A2E and iso-A2E fluorescence is scarcely evident. At the same time, as discussed above,  $A2E_{ox,deg}$ -group emission



mainly contributes to total fluorescence (Figs. 3b,c, chromatograms 2 and 3; Table 3).

Emissions detected at wavelengths of 600 and 650 nm (Fig. 3b, chromatogram 3; Fig. 3c, chromatograms 2 and 3)

result in quite broad and intense peaks (possibly from several products) occurring during the 6th to 7th minute of the chromatogram measurement. Hence, in this time interval, this product (or several products) appears as chromatogram noise

**Table 2** Relative content of LG fluorophores detected in chloroform extract from human RPE in separate groups<sup>a</sup>

Wavelength of detection (nm)	A2E <sub>ox,deg</sub> (%)	A2E and iso-A2E (%)	A2E <sub>mod</sub> (%)
340	57.48±3.21	18.27±1.22	24.24±0.12
430	40.01±2.02	28.31±1.01	31.68±1.31
510	28.84±0.98	25.15±0.75	46.01±1.45

<sup>a</sup>Data were calculated from chromatograms in Fig. 3 (a, b, and c, chromatograms 1)

detected by absorption at different wavelengths (Figs. 3b,c, chromatogram 1).

Thus, HPLC analysis of the fluorescent properties of individual components in the RPE chloroform extract reveals that the A2E<sub>ox,deg</sub> group fluorophores make the highest relative contribution to the total fluorescence of the extract.

Relative content of fluorophores in chloroform extract from cadaver eyes without signs of pathology, obtained from donors of different ages

In this series of experiments, 42 individual samples of suspended RPE cells without signs of pathology, extracted from cadaver eyes of donors aged from 17 to 78 years, were obtained and studied. For each sample, the fluorescence spectrum excited by radiation at a wavelength of 430 nm was recorded. Irrespective of the donor age, fluorescence-spectrum maxima were located within the range 575±15 nm (data not shown).

A chloroform extract for HPLC analysis was obtained from every suspended-RPE-cell sample. The HPLC analysis was performed with absorption detection at a

**Table 3** Relative contribution of fluorescence intensity of fluorophore groups in chloroform extract from human RPE to total fluorescence of all detectable products<sup>a</sup>

Emission (nm)	A2E <sub>ox,deg</sub> (%)	A2E and iso-A2E (%)	A2E <sub>mod</sub> (%)
Excitation by 340 nm			
500	96.17±3.46	0.74±0.03	2.61±0.23
600	81.53±2.13	1.97±0.01	16.50±1.02
Excitation by 430 nm			
500	97.26±3.67	0.08±0.01	2.66±0.11
600	81.24±1.05	1.67±0.14	17.08±1.02
Excitation by 510 nm			
600	96.27±2.37	0.99±0.04	2.72±0.24
650	91.97±1.29	–	8.03±0.71

<sup>a</sup>Data were calculated from chromatograms in Fig. 3 (a, b, and c, chromatograms 2 and 3)

wavelength of 430 nm. Figure 4a shows a typical HPLC chromatogram for the RPE chloroform extract of an individual cadaver eye without signs of pathology. Peaks or groups of peaks 1–5 correspond to A2E<sub>ox,deg</sub>; peaks 6 and 8 correspond to A2E and iso-A2E, respectively; the group of peaks 11 may correspond to products identified in [18–20].

For statistical processing of the results, data were combined into groups on the basis of age. In total, six groups of samples (1, 2, 3, 4, 6, and 8) without signs of pathology were combined. The relative content of individual fluorophores or groups of fluorophores in the chloroform extract from RPE cells under study was determined from HPLC data (Fig. 4b (gray columns) and Table 4). The relevant trace reveals that the relative content of A2E itself (peak 6) and A2E<sub>ox,deg</sub> (peaks and/or groups of peaks 1–5) increases with donor age. An abrupt decrease in the relative content of iso-A2E in the chloroform extract (peak 8) with increase in donor age remains unexplained. This phenomenon has already been reported [10].

Note that the age-related increase in the relative contents of most products, and of both A2E and A2E<sub>ox,deg</sub>, is almost linear (Fig. 4b). However, if iso-A2E is included in the calculation of the A2E<sub>ox,deg</sub>/A2E ratio (i.e. A2E<sub>ox,deg</sub>/(A2E + iso-A2E)), the latter increases from 0.69±0.03 to 1.32±0.04 with donor age (Fig. 4c, Table 5).

Relative content of fluorophores in RPE chloroform extract from cadaver eyes with signs of AMD

In two cases of post-mortem inspection of eyecups of cadaver eyes by an ophthalmologist, AMD signs in RPE were detected. Figure 5a shows images of the fundus after retina removal without and with signs of AMD. For normal eyes, the RPE is uniform, without focal abnormalities; the foveolar area has more-intense pigmentation of RPE cells. In the fundus with AMD signs, the RPE is uneven and there is redistribution of the pigment in the paramacular area; multiple drusen-like deposits are present, which are yellowish colored with irregular borders and are rather prominent, surrounded by a hyperpigmentation area.

For comparative analysis, cadaver eyes with and without signs of AMD were taken from similarly aged donors. Figures 5b,c show that if the RPE has signs of pathology, the fluorescence-spectrum maxima of the suspended cells are shifted noticeably towards the short-wave region compared with samples obtained from cadaver eyes with no pathology. For the first 1 (norm)–2 (pathology) pair, the difference in fluorescence-maxima locations is more noticeable: 564 and 528 nm, respectively. For the second 3 (norm)–4 (pathology) pair, the



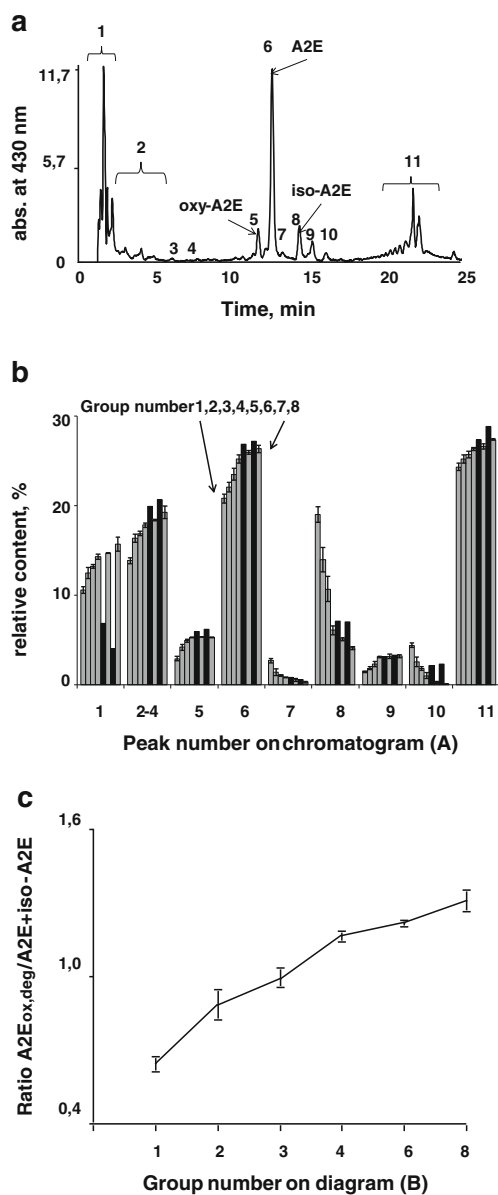


**Fig. 4** Relative content of LG fluorophores in chloroform extracts from RPE human-cadaver eyes without signs of pathology, obtained from donors of different ages, and, in two cases, from cadaver eyes with signs of AMD. HPLC analysis of chloroform extract from RPE obtained from one cadaver eye (**a**) (donor aged 51 years, fundus of eye without pathology). Absorption detection at 430 nm. Peaks 1–5, A2E<sub>ox,deg</sub> (A2E photo-oxidation and photodegradation products); peaks 6 and 8, A2E and iso-A2E, respectively; the group of peaks 11 may correspond to products identified in Refs. [18–20]. Relative content of detected fluorophores or fluorophore groups in chloroform extracts from RPE (**b**). Samples were obtained from 42 cadaver eyes and analyzed by HPLC (reversed-phase, C<sub>18</sub> column with monitoring at 430 nm). For statistical analysis, data on the relative content of the individual products in the RPE extract analyzed were combined into eight groups by age. Group 1: 17 years (*n*=4), 20 years (*n*=2), 22 years (*n*=3), 24 years (*n*=2), and 27 years (*n*=1); group 2: 30 years (*n*=1), 34 years (*n*=1), 35 years (*n*=2), 37 years (*n*=2), 38 years (*n*=1), and 39 years (*n*=1); group 3: 40 years (*n*=2), 45 years (*n*=2), and 48 years (*n*=2); group 4: 51 years (*n*=3), 54 years (*n*=1), 57 years (*n*=1), and 59 years (*n*=1); group 5: 58 (*n*=1), signs of pathology; group 6: 60 years (*n*=1), 61 years (*n*=1), 65 years (*n*=1), and 67 years (*n*=2); group 7: 70 (*n*=1), signs of pathology; group 8: 70 years (*n*=2), and 78 years (*n*=3). *Gray columns*, no signs of pathology; *black columns*, signs of pathology; *x-axis*, numbers of peaks represented on panel **a**; *y-axis*, relative content of fluorophores or fluorophore groups detected in chloroform extract (%). The percentage of components in the mixture was calculated from the ratio of the component surface area to total surface area of all peaks on chromatogram, i.e., the relative content of components. Dependence of the A2E<sub>ox,deg</sub>/(A2E + iso-A2E) ratio on donor age (**c**). Ratio was calculated from data represented on panel **b** for samples obtained from cadaver eyes with no signs of pathology

locations are 563 and 540 nm, respectively. In samples with signs of pathology, this shift of fluorescence maxima to the shortwave region may indicate increased content of A2E<sub>ox,deg</sub> in LGs.

Chloroform extracts were obtained from suspensions of RPE cells of analyzed samples, and the composition of fluorophores and their relative content were analyzed by HPLC (Fig. 5 and Table 4). Comparative HPLC analysis of the chloroform extracts revealed different relative contents of LG fluorophores in RPE cadaver eyes without and with signs of pathology. For fraction 1 on the chromatograms (2 and 4; pathology), samples obtained from cadaver eyes with signs of AMD have a more diversified set of peaks, although their relative content is almost twofold lower (Fig. 4b (black columns) and Table 4). An increase

in the relative content of fraction 2 components and relative content of A2E (peak 6) is also observed (Fig. 4b (black columns) and Table 4).

Thus, samples obtained from cadaver-eye RPE with signs of AMD deviate from the norm both in location of the fluorescence maximum of suspended RPE cells and in relative content of virtually all products detectable in HPLC analysis of RPE chloroform extract.

## Conclusion

This work studied changes in spectral properties and composition of human LG fluorophores with age and pathology. A special focus was the fluorescent properties of photo-oxidation products of both synthetic A2E and LG fluorophores extracted from the RPE of human-cadaver eyes. How the ratio of oxidized to unoxidized fluorophores changes with age was also studied. In addition, inspection by an ophthalmologist identified two cadaver eyes with signs of AMD in the RPE, from donors aged 58 and 70 years. Thus a comparative analysis of the spectral characteristics and composition of LG fluorophores from cadaver eyes with and without signs of AMD was performed.

**Table 4** Dependence of relative content (%) of fluorophores in RPE chloroform extract of cadaver eyes without and with signs of AMD in the RPE on the basis of donor age<sup>a</sup>

Peak no. in Fig. 4	Group number in Fig. 4b, and age							
	1 17–29 yr.	2 30–39 yr.	3 40–49 yr.	4 50–59 yr.	5 58 yr.	6 60–69 yr.	7 70 yr.	8 70–79 yr.
1	10.6±0.4	12.5±0.6	13.2±0.2	14.3±0.3	6.9	14.7±0.1	4.0	15.7±0.8
2–4	13.8±0.3	16.4±0.5	16.9±0.3	17.8±0.3	19.9	18.4±0.1	20.7	19.2±0.7
5	2.9±0.3	4.2±0.3	4.9±0.2	5.3±0.1	5.9	5.3±0.1	6.2	5.3±0.1
6	20.8±0.5	22.0±0.6	23.5±0.7	25.2±0.5	26.9	25.9±0.2	27.2	26.3±0.4
7	2.7±0.3	1.4±0.4	1.0±0.1	0.9±0.1	0.8	0.6±0.2	0.5	0.3±0.1
8	19.0±1.0	13.9±1.4	10.7±1.4	6.1±0.5	7.1	5.1±0.2	7.0	4.1±0.2
9	1.5±0.1	1.9±0.2	2.3±0.3	3.1±0.1	3.1	3.2±0.2	3.3	3.2±0.2
10	4.4±0.3	2.5±0.5	1.8±0.2	1.0±0.3	2.2	0.3±0.1	2.3	0.1±0.1
11	24.3±0.4	25.2±0.4	25.7±0.7	26.3±0.2	27.3	26.6±0.3	28.8	27.4±0.1

<sup>a</sup> Each group number corresponds to the column number (gray and black) in Fig. 4b. The peak number corresponds to the peak number in Fig. 4a. For statistical analysis, data on the relative content of the individual products in the RPE extract analyzed were divided into groups on the basis of age. Group 1: 17 years ( $n=4$ ), 20 years ( $n=2$ ), 22 years ( $n=3$ ), 24 years ( $n=2$ ), and 27 years ( $n=1$ ); group 2: 30 years ( $n=1$ ), 34 years ( $n=1$ ), 35 years ( $n=2$ ), 37 years ( $n=2$ ), 38 years ( $n=1$ ), and 39 years ( $n=1$ ); group 3: 40 years ( $n=2$ ), 45 years ( $n=2$ ), and 48 years ( $n=2$ ); group 4: 51 years ( $n=3$ ), 54 years ( $n=1$ ), 57 years ( $n=1$ ), and 59 years ( $n=1$ ); group 6: 60 years ( $n=1$ ), 61 years ( $n=1$ ), 65 years ( $n=1$ ), and 67 years ( $n=2$ ); group 8: 70 years ( $n=2$ ), and 78 years ( $n=3$ ). Results from samples obtained from human cadaver eyes with signs of AMD in the RPE are shown in Table 4, columns 5 and 7

The results reveal that the fluorescence maximum of suspended RPE cells from human-cadaver eyes with no signs of pathology is independent of donor age and lies in the range  $575\pm 15$  nm. In contrast, the study reveals that the ratio of oxidized to unoxidized LG fluorophores does change with age. In particular, the ratio  $A2E_{ox,deg}/(A2E + iso-A2E)$  increases from  $0.69\pm 0.03$  to  $1.32\pm 0.04$ . It is possible that increasing levels of photooxidation and photodegradation products within RPE cells with age particularly raise the risk of AMD.

This work reveals that the fluorescence properties of individual components in the RPE chloroform extract do not correlate with their absorption at a specific wavelength. For instance, A2E content is the highest of all individual products detectable by absorption at wavelengths of 430 and 510 nm. However, when fluorescence is excited by radiation, very low emission by this

product at wavelengths of 500, 600, and 650 nm is observed (Fig. 3). The highest relative contribution to total fluorescence is  $A2E_{ox,deg}$  products detected at initial retention times. It is possible that the fluorescent properties of individual LG fluorophores vary greatly after their extraction into chloroform and, hence, on separation in the chromatographic column. Nevertheless, it is clear that the A2E contribution to total fluorescence of the chloroform extract (in vitro) is too low, and it is probable that the contribution of A2E to the pattern of fundus AF (in vivo) is also quite low. There are also occasional statements in the literature that A2E is a small component of the lipofuscin in the human RPE [33].

Defined differences in fluorescence properties between chloroform extracts from cadaver eyes with and without signs of AMD are discussed here for the first time. These observations hold promise for the future

**Table 5**  $A2E_{ox,deg}/(A2E+iso-A2E)$  ratio with respect to donor age<sup>a</sup>

$\Sigma$ peaks in Fig. 4a	Group number in Fig. 4b					
	1 17–29 years	2 30–39 years	3 40–49 years	4 50–59 years	6 60–69 years	8 70–79 years
$\Sigma(1-5)$ $A2E_{ox,deg}$ (%)	27.32±0.74	32.99±1.31	35.01±0.51	37.39±0.31	38.41±0.08	40.18±0.81
$\Sigma(6,8)$ $A2E + iso-A2E$ (%)	39.79±0.78	36.01±0.85	34.17±0.79	31.29±0.31	30.99±0.17	30.44±0.55
$A2E_{ox,deg}/A2E+iso-A2E$	0.69±0.03	0.92±0.06	1.02±0.04	1.19±0.02	1.24±0.01	1.32±0.04

<sup>a</sup> Ratios were calculated from data listed in Table 4 for samples obtained from cadaver eyes with no signs of pathology

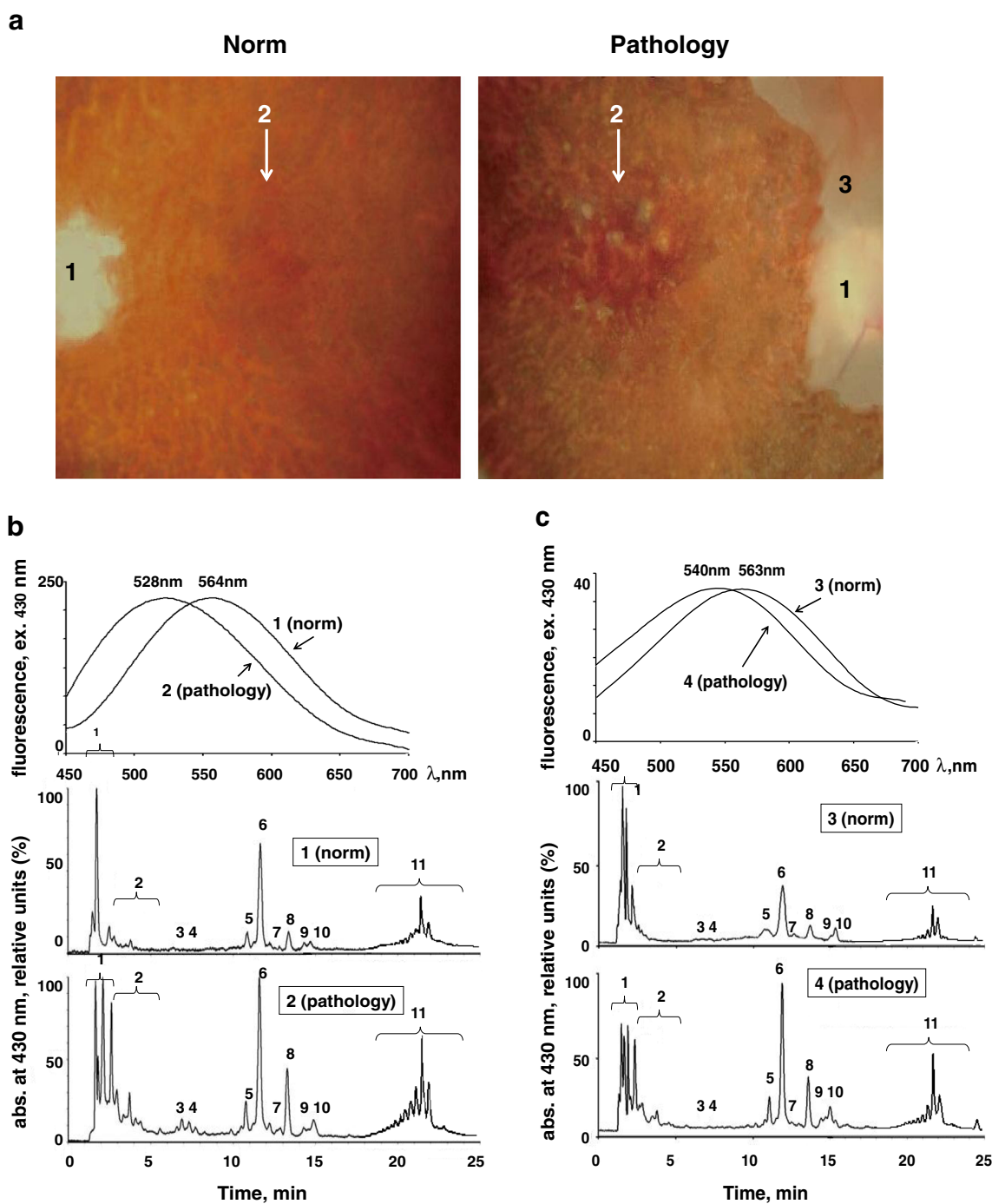


**Fig. 5** Comparative analysis of spectral characteristics and composition of LG fluorophores from RPE human-cadaver eyes with and without signs of AMD. Images of human-cadaver-eye fundus after retina removal (**a**): donor aged 59 years, fundus of eye without pathology (*Norm*); donor aged 58 years, fundus of eye with signs of AMD (*Pathology*). 1, disk of optic nerve; 2, macular area; 3, retina fragments. Comparative analysis of spectral characteristics of RPE cell suspensions and composition of LG fluorophores from cadaver eyes with and without signs of AMD (**b** and **c**). Fluorescence emission spectra of RPE cell suspensions from

individual cadaver eyes were recorded. Excitation was performed by radiation at 430 nm. Spectra were normalized. HPLC analysis of chloroform extracts from RPE cell suspensions was performed with monitoring absorption at 430 nm. The samples were obtained from cadaver eyes of four different donors. First pair (**b**): donor aged 59 years, fundus of eye without pathology (1) and donor aged 58 years, fundus of eye with signs of AMD (2); second pair (**c**): donor aged 65 years, fundus of eye without pathology (3) and donor aged 70 years, fundus of eye with signs of AMD (4)

development of AF imaging. Further in-depth study of the fluorescent properties of A2E<sub>ox,deg</sub> products, and

determination of their accumulation with age and in the presence of pathology, is warranted.

**Acknowledgements** The work was supported by the Basic Research Program of the Russian Academy of Sciences “Basic Science Applications to Medicine”, the Russian Foundation for Basic Research (No. 12-04-00844). The part of research related to mass spectrometry measurements was supported by the Russian Scientific Fund (Grant 14-24-00114).

**Conflict of interest** The authors declare that there is no conflict of interest regarding the publication of this paper.

## References

- Schmitz-Valckenberg S, Holz FG, Bird AC, Spaide RF (2008) Fundus autofluorescence imaging. *Retina* 28:385–409
- Geng L, Wihlmark U, Algvare PV (1999) Lipofuscin accumulation in iris pigment epithelial cells exposed to photoreceptor outer segments. *Exp Eye Res* 69:539–546
- Lois N, Holder GE, Bunce C, Fitzke FW, Bird AC (2001) Phenotypic subtypes of Stargardt macular dystrophy-fundus flavimaculatus. *Arch Ophthalmol* 119:359–369
- von Ruckmann A, Fitzke FW, Bird AC (1997) In vivo fundus autofluorescence in macular dystrophies. *Arch Ophthalmol* 115:609–615
- Kennedy CJ, Rakoczy PE, Constable IJ (1995) Lipofuscin of the retinal pigment epithelium: a review. *Eye* 9:763–771
- Holz FG, Fleckenstein M, Schmitz-Valckenberg S, Bird AC (2007) Evaluation of fundus autofluorescence images. In: Holz FG, Schmitz-Valckenberg S, Spaide RF, Bird AC (eds) *Atlas of fundus autofluorescence imaging*. Springer-Verlag, Berlin
- Boulton M, Dontsov A, Jarvis-Evans J, Ostrovsky M, Svistunenko D (1993) Lipofuscin is a photoinducible free radical generator. *J Photochem Photobiol B Biol* 19:201–204
- Ben-Shabat S, Itagaki Y, Jockusch S, Sparrow JR, Turro NJ, Nakanishi K (2002) Formation of a nonaioxirane from A2E, a lipofuscin fluorophore related to macular degeneration, and evidence of singlet oxygen involvement. *Angew Chem Int Ed* 42:814–817
- Schmitz-Valckenberg S, Holz FG, Fitzke FW (2007) Perspectives in imaging technologies. In: Holz FG, Schmitz-Valckenberg S, Spaide RF, Bird AC (eds) *Atlas of fundus autofluorescence imaging*. Springer-Verlag, Berlin
- Feldman TB, Yakovleva MA, Dontsov AE, Ostrovsky MA (2010) Fluorescence emission and excitation spectra of fluorophores of lipofuscin granules isolated from retinal pigment epithelium of human cadaver eyes. *Russ Chem Bull, Int Ed* 59:276–83 (Published in Russian in *Izvestiya Akademii Nauk. Seriya Khimicheskaya* (2010) 1:269–276)
- Eldred GE, Katz ML (1988) Fluorophores of the human retinal pigment epithelium: separation and spectral characterization. *Exp Eye Res* 47:71–86
- Sparrow JR, Wu Y, Kim CY, Zhou J (2009) Phospholipid meets all-*trans*-retinal: the making of RPE bisretinoids. *J Lipid Res* 51:247–261
- Sakai N, Decatur J, Nakanishi K, Eldred GE (1996) Ocular age pigment “A2E”: an unprecedented pyridinium bisretinoid. *J Am Chem Soc* 118:1559–1560
- Lamb LE, Simon JD (2004) A2E: a component of ocular lipofuscin. *Photochem Photobiol* 79:127–136
- Sparrow JR, Kim SR, Cuervo AM, Bandhyopadhyay U (2008) A2E, a pigment of RPE lipofuscin, is generated from the precursor, A2PE by a lysosomal enzyme activity. *Adv Exp Med Biol* 613:393–398
- Parish CA, Hashimoto M, Nakanishi K, Dillon J, Sparrow JR (1998) Isolation and one-step preparation of A2E and iso-A2E, fluorophores from human retinal pigment epithelium. *Proc Natl Acad Sci U S A* 95:14609–14613
- Ben-Shabat S, Parish CA, Vollmer HR, Itagaki Y, Fishkin N, Nakanishi K, Sparrow JR (2002) Biosynthetic studies of A2E, a major fluorophore of retinal pigment epithelial lipofuscin. *J Biol Chem* 277:7183–7190
- Kim SR, Jang YP, Jockusch S, Fishkin NE, Turro NJ, Sparrow JR (2007) The all-*trans*-retinal dimer series of lipofuscin pigments in retinal pigment epithelial cells in a recessive Stargardt disease model. *Proc Natl Acad Sci U S A* 104:19273–19278
- Wu Y, Fishkin NE, Pande A, Pande J, Sparrow JR (2009) Novel lipofuscin bisretinoids prominent in human retina and in a model of recessive Stargardt disease. *J Biol Chem* 284:20155–20166
- Sparrow JR, Wu Y, Nagasaki T, Yoon KD, Yamamoto K, Zhou J (2010) Fundus autofluorescence and the bisretinoids of retina. *Photochem Photobiol Sci* 9:1480–1489
- Yamamoto K, Yoon KD, Ueda K, Hashimoto M, Sparrow JR (2011) A novel bisretinoid of retina is an adduct on glycerophosphoethanolamine. *Invest Ophthalmol Vis Sci* 52:9084–9090
- Yoon KD, Yamamoto K, Ueda K, Zhou J, Sparrow JR (2012) A novel source of methylglyoxal and glyoxal in retina: implications for age-related macular degeneration. *PLoS One* 7:e41309, <http://www.plosone.org>
- Wu Y, Yanase E, Feng X, Siegel MM, Sparrow JR (2010) Structural characterization of bisretinoid A2E photocleavage products and implications for age-related macular degeneration. *Proc Natl Acad Sci U S A* 107:7275–7280
- Wang Z, Keller LMM, Dillon J, Gaillard ER (2006) Oxidation of A2E results in the formation of highly reactive aldehydes and ketones. *Photochem Photobiol* 82:1251–1257
- Eldred GE, Lasky MR (1993) Retinal age pigments generated by self-assembling lysosomotropic detergents. *Nature* 361:724–726
- Sparrow JR, Boulton M (2005) RPE lipofuscin and its role in retinal pathobiology. *Exp Eye Res* 80:595–606
- Kim SR, Jang Y, Sparrow JR (2010) Photooxidation of RPE lipofuscin bisretinoids enhances fluorescence intensity. *Vision Res* 50:729–736
- Yakovleva MA, Feldman TB, Krupennikova AS, Borzenok SA, Ostrovsky MA (2010) Fluorophores of lipofuscin granules responsible for human eye fundus autofluorescence. *Russ Chem Bull, Int Ed* 59:2309–2317 (Original Russian Text published in *Izvestiya Akademii Nauk. Seriya Khimicheskaya* (2010) 12:2252–2260)
- Russian Federation law N 4180-I dated 22.12.1992, “On human organs or tissue transplantation” (with modifications and additions). <http://base.garant.ru/136366/>
- Folch J, Lees M, Stanley GHS (1957) A simple method for the isolation and purification of total lipids from animal tissues. *J Biol Chem* 226:497–509
- Yakovleva MA, Sakina NL, Kononikhin AS, Feldman TB, Nikolaev EN, Dontsov AE, Ostrovsky MA (2006) Detection and Study of the Products of Photooxidation of *N*-Retinylidene-*N*-retinylethanolamine (A2E), the Fluorophore of Lipofuscin Granules from Retinal Pigment Epithelium of Human Donor Eyes. *Dokl Biochem Biophys* 409:223–225 (Original Russian Text published in *Doklady Akademii Nauk* (2006) 409:411–414)
- Dillon JP, Wang Z, Avallé LB, Gaillard ER (2004) The photochemical oxidation of A2E results in the formation of a 5,8,5',8',-bis-furanoid oxide. *Exp Eye Res* 79:537–542
- Krogmeier JR, Clancy CM, Pawlak A, Rozanowska M, Sarna T, Simon JD, Dunn RC (2001) Mapping the distribution of emissive molecules in human ocular lipofuscin granules with near-field scanning optical microscopy. *J Microsc* 202:386–390



**Tatiana B. Feldman** is Ph.D. in biophysics, Dr Sc., and a docent in the Molecular Physiology Department, Biological Faculty, Lomonosov Moscow State University, and a senior researcher in the Laboratory of Physical and Chemical Bases of Vision in the Emanuel Institute of Biochemical Physics of the Russian Academy of Sciences. Her current scientific interests focus on the molecular physiology of vision in normal and pathological conditions: femtosecond spectroscopy of rhodopsin;

spectral properties and composition of lipofuscin fluorophores from human retinal pigment epithelium; vision of invertebrates.



**Sergey A. Borzenok** is Ph.D., Dr Sc., Professor, M.D., ophthalmologist, and head of the Center for Fundamental and Applied Biomedical Problems of the Sv. Fyodorov Eye Microsurgery Complex. With the support of Academician S.N. Fedorov he founded the first eye bank in Russia. He is a member of the relevant committee of the Expert Council on Transplantation of the Russian Federation. His research interests are clinical and experimental ophthalmology, cellular biology, genomic pathology, pathological and molecular physiology, immunology, transplantation, and artificial organs.

nomical pathology, pathological and molecular physiology, immunology, transplantation, and artificial organs.



**Marina A. Yakovleva** is Ph.D., and a researcher in the Laboratory of Physical and Chemical Bases of Vision in the Emanuel Institute of Biochemical Physics of the Russian Academy of Sciences. She is a specialist in HPLC and fluorescence-spectroscopy methods. She is investigating spectral properties of lipofuscin-granule fluorophores in retinal pigment epithelium of human eyes.



**Alexey S. Kononikhin** is Ph.D. in chemical physics. He is a deputy head of the Laboratory of Ion and Molecular Physics Department at the Moscow Institute of Physics and Technology and a leading researcher at the Institute for Energy Problems of Chemical Physics. His research interests include applications of high-resolution mass spectrometry in chemistry, biology, and medicine, including proteomics of the human body under extreme conditions.



**Patimat M. Arbukhanova** is Ph.D., M.D., ophthalmologist, and junior researcher of the Center for Fundamental and Applied Biomedical Problems of the Sv. Fyodorov Eye Microsurgery Complex. Her scientific work is devoted to investigation of the spectral characteristics of lipofuscin granules of the retinal pigment epithelium in normal and pathological fundus. Her research interest is fundamental investigation of ophthalmology, cell biology, and retinal pigment epithelium

cells from cadaver donor's eyes: selection, isolation, and cultivation, and molecular physiology and pathology of vision.



**Igor A. Popov** is Ph.D. in chemical physics. He is a chair of the Molecular Physics Department and a head of laboratory at the Moscow Institute of Physics and Technology. He is a leading researcher in the Laboratory of Mass spectrometry of Biomacromolecules at the Emanuel Institute of Biochemical Physics of the Russian Academy of Sciences. His research interests include applications of high-resolution mass spectrometry in chemistry, biology, and medicine, including proteomics of the human body under extreme conditions.

ogy, and medicine, including proteomics of the human body under extreme conditions.



**Evgeny N. Nikolaev** is Ph.D. in chemical physics, Dr Sc., Professor, head of the Laboratory of Ion and Molecular Physics in the Institute for Energy Problems of Chemical Physics Russian Academy of Sciences, and head of the Laboratory for Mass Spectrometry of Biomacromolecules in the Emanuel Institute of Biochemical Physics Russian Academy of Sciences. Areas of specialization: mass-spectrometry of biomolecules, computer sciences, proteomics. Current research activities: supercomputer modeling of ion-cloud behavior in accumulation and transport mass-spectrometer devices; investigation of the body-liquid proteome of healthy men by accurate mass-retention-time method using FT-ICR mass spectrometry; development of fundamental bases for quantitative mass-spectrometry approaches to investigation of middle-copy human proteins; classification analysis of organic-carbon natural storages using ultrahigh-accuracy mass spectrometry

(Fourier-transform ion-cyclotron-resonance mass spectrometry); development and characterization of dynamically harmonized Penning traps for FT-ICR MS.



**Mikhail A. Ostrovsky** is Ph.D. in physiology, Dr Sc., Professor, a physiologist, and is known internationally for his work in vision and biology. He is a Full Member (Academician) of the Russian Academy of Sciences, a Professor of Lomonosov Moscow State University, and President of the Pavlov Physiological Society of Russia. He is Head of Laboratory at the Emanuel Institute of Biochemical Physics, Russian Academy of Sciences and Head of Department

of Molecular Physiology at the Biological Faculty of Lomonosov Moscow State University.